APPLIED ORGANOMETALLIC CHEMISTRY
Appl. Organometal. Chem. 2001; **15**: 421–429
DOI: 10.1002/aoc.164

Synthesis of ultrafine titanium carbonitride powders†

Frederic Monteverde,* Valentina Medri and Alida Bellosi
CNR–IRTEC, Research Institute for Ceramics Technology Via Granarolo 64, 48018 Faenza (Ra), Italy

Titanium-carbonitride-based materials are very hard materials with increasing technical importance. They are mainly used in composites with various metal carbides and/or metallic binders (cermets) for metal cutting operations. These applications call for the synthesis of titanium carbonitride powders with homogeneous chemical composition, as small as possible grain size and narrower grain size distribution. Nowadays on the market, only commercial submicrometric (0.5–2 μm) powders are available. Starting from blends of nanosize commercial TiN or TiO_2 powders mixed with different carbon powders (carbon black, active carbon), this study aimed to set up a low-cost process to synthesize fine and pure $TiC_{1-X}N_X$ powders with an X value close to 0.5. The morphology of the as-obtained powders and the progress of the reaction were investigated by scanning electron microscopy and X-ray diffraction. The stoichiometric parameter X was estimated on the basis of a $TiC_{1-X}N_X$ Raoultian solid solution together with Vegard's rule. The results are presented and discussed to assess relations between powder characteristics and processing conditions. The most encouraging results were obtained using a mixture TiN + 10 wt% C (carbon black) processed at 1430 °C for 3 h under flowing argon. Regularly shaped particles with limited agglomeration ranged from 100 to 300 nm and an X value close to 0.5 Copyright © 2001 John Wiley & Sons, Ltd.

Keywords: structural materials; ceramic powders; carbothermal reduction; carbonitridation; high-temperature synthesis; SEM; XRD; reaction mechanisms

INTRODUCTION

Carbides, nitrides or solid solutions of transition metals (e.g. titanium carbonitride (TiCN)) are known for their outstanding properties, such as high melting point and thermal conductivity, significant hardness–toughness compromise, good oxidation and wear resistance, and low electrical resistivity. Therefore, they are widely used for the preparation of advanced engineering ceramic-based composites employed in several applications in key high technologies; metal working, electrical/electronic/automative/refractory industries.[1–12]

These applications are therefore calling evermore for the synthesis of powders with homogeneous composition, small grain size and narrow grain size distribution. The features mentioned ensure the reduction of heterogeneity from the initial powder mixture.

In particular, TiCN is employed for continuous casting of steel, provides better adhesion with metallic substrates and improves oxidation resistance (e.g. coated tip of cutting tool, thermal barrier coating), and strengthens ferrous matrices for wear-resistant surfaces.[3]

The more usual routes to produce TiCN powders are:

- synthesis by high-temperature solid-state diffusion from TiN–TiC, TiN–C, TiC–Ti powder blends;[2]
- carbothermal reduction and simultaneous carbonitridation from TiO_2[2,3,5–11] or sol–gel precursors;[13]
- thermal decomposition of $TiCl_4$–amine (or nitrile) complexes.[1]

The carbothermal reduction is largely recognized as a low-cost method for the synthesis of non-oxide ceramic powders, i.e. carbides and nitrides of transition metals, with a fairly simple processing set-up, wide range of C/N ratios and potentially mass-scale production.

Starting from mechanically mixed powder samples, and considering that they constitute a

* Correspondence to: F. Monteverde, CNR–IRTEC, Research Institute for Ceramics Technology, Via Granarolo 64, 48018 Faenza (Ra), Italy.
E-mail: federico@irtec1.irtec.bo.cnr.it
† Based on work presented at the 1st Workshop of COST 523: Nanomaterials, held at Frascati, Italy, 20 October 1999.
Contract/grant sponsor: MURST.
Contract/grant sponsor: CNR.

randomly separated particle array, the extent of the reaction is often limited by the contact area among the reactants. Sometimes, such a deficiency causes unfinished reactions or undesired products. Sol–gel techniques offer the advantages to prepare very homogeneous and highly reactive starting mixtures, but an additional treatment of pyrolysis and crystallization is needed before the onset of the carbothermal reduction itself.[13] In any case, the substitution rate of oxygen by carbon and nitrogen within the initial TiO_2 lattice is low. Thus, procedures different from conventional mechanical dry mixing of powders and their subsequent carbothermal reduction/carbonitridation do not seem to be competitive in terms of quality/cost for the production of ultrafine pure TiCN powders.

The literature reports on several attempts to clarify the mechanism involved during the previously mentioned reactions, but real or sometimes only apparent contradictions in the experimental results have led to different interpretations that are still a matter of discussion.[2,3,5,7–10,12,13]

Starting from blends of nanosize commercial TiN or TiO_2 powders mixed with different carbon powders (two carbon blacks, one active carbon), this study aimed to set up a low-cost route to synthesize pure and as fine as possible $TiC_{1-X}N_X$ powders with an X value close to 0.5. The relationships among raw powders, processing conditions and characteristics of the products are reported and discussed.

DESCRIPTION OF THE TiCN PHASE

The $TiC_{1-X}N_X$ compound can be simply drawn as a $TiC_{1-X} - TiN_X$ Raoultian solid solution, $0 \leq X \leq 1$, with a B1-NaCl crystal lattice in which the non-metallic sublattice sites are randomly occupied by carbon and nitrogen atoms.[2,3,14] Actually, this model does not take account of the total vacancy concentration within the lattice. In order to include it, the cell parameter of a non-stoichiometric $TiC_{1-X} - TiN_X$ must be considered. Moreover, the two interstitial compounds TiN and TiC do not mix ideally, but exhibit a small negative departure from Raoultian behaviour. Since oxygen can be reasonably thought of as always present whatever the processing route, and TiO forms a pseudoternary solid solution with TiN and TiC (i.e. mutual exchange of carbon, nitrogen and oxygen at the interstitial sites), it is more correct to speak of synthesis in the TiO–TiN–TiC system.[3] The slight negative departure from a Raoultian TiN–TiC solid solution becomes non-negligible when more oxygen atoms occupy interstitial sites: the TiC–TiN–TiO solid solution shifts much more from the ideal behaviour.[4]

EXPERIMENTAL SET-UP

Target

The characterization of all the mixtures processed was focused mainly on the optimization of a process to achieve a combination of desired features in the final powder. In particular, several tests were performed in order to tune a low-cost experimental set-up able to obtain a pure (no carbon residue), ultrafine (i.e. grain size less than 0.2 μm) $TiC_{1-X}N_X$ phase with a controlled granulometric distribution, little agglomeration and the parameter X close to 0.5.

Powder processing

The characteristics of the commercial nanosize powders used are reported in Table 1. For the compositions (a) TiN +10 wt% C and (b)

Table 1 Characteristics of the starting powders

Powder	Company	Specific surface area ($m^2\ g^{-1}$)	Impurities (wt%)	Notes
TiN	HC Starck	24.6	O, 0.68; Cl, 0.5; C, 0.08	—
TiO_2	Rhone–Poulenc	87	sulfate 0.5	—
C-1	Degussa	113	—	Carbon black
C-2	—	23	—	Carbon black
C-3	Merck	—	—	Active carbon

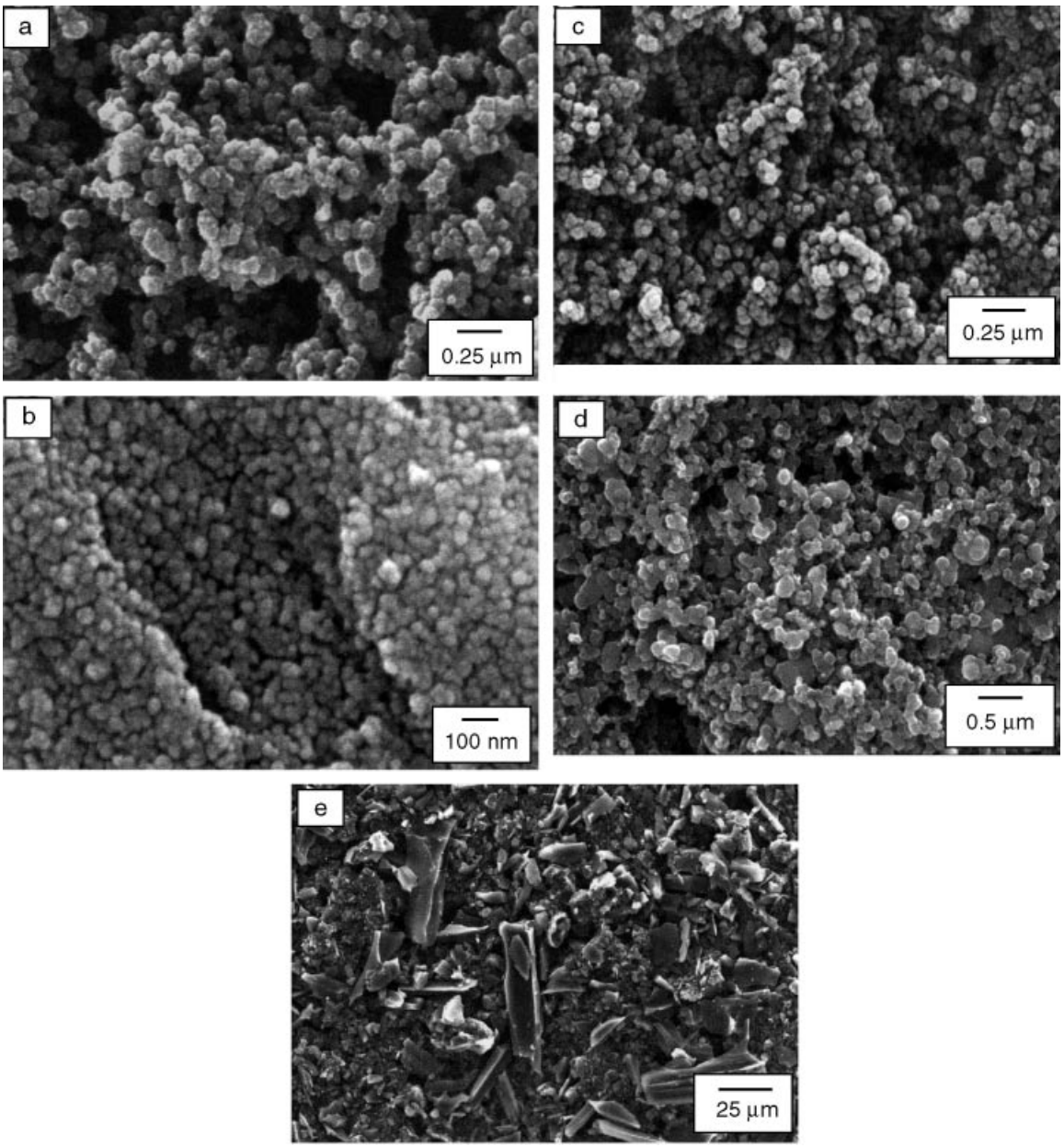

Figure 1 SEM micrographs of commercial TiN (a), TiO_2 (b), carbon black 1 (c), carbon black 2 (d), and active carbon 3 (e).

$TiO_2 + 27$ wt% C, six different mixtures (three each for TiN and TiO_2) were wet mixed in *n*-hexane by ultrasonification, dried with a rotating evaporator, sieved and finally pelletized ($\sim$1 g, 1000 kg cm^{-2}). The series of micrographs (Fig. 1) depicts the morphology of the powders employed.

The high-temperature synthesis from TiN/C mixtures in flowing argon and the carbothermal reduction and simultaneous carbonitridation of TiO_2/C blends were investigated by scheduling a sequence of thermal cycles from 1300 to 1700 °C (heating rate 10 °C min^{-1}, free cooling down) in a

graphite crucible with a heated graphite chamber, carefully purged with inert gas before heating. The isothermal step ranged from 30 min up to 4 h.

All the mixtures processed were weighed before and after treatment, pestled in an agate mortar and analysed by X-ray diffraction (XRD) to estimate X and by scanning electron microscopy (SEM) to evaluate morphology, grain size, and necking–coarsening effects.

The TiCN phase was modelled as a perfect TiC_{1-X} – TiN_X solid solution, $0 \leq X \leq 1$, with a B1-NaCl type crystal lattice.[14] In accordance with Vegard's rule,

$$a_{TiCN} = (X_C a_{TiC}) + (X_N a_{TiN}) \quad [1]$$

where $X_C = 1 - X_N$, $a_{TiC} = 0.43274$ nm (ICDD card 32-1383), $a_{TiN} = 0.42417$ nm (ICDD card 38-1420). The atomic percentage of the carbon and nitrogen atoms was estimated from the cell parameter a_{TiCN}, being extrapolated from XRD patterns with the Nelson–Riley function.[15]

The oxygen content and the specific surface area were measured, respectively, by the LECO and BET method only on selected products. The progress of the reactions was monitored in terms of weight change and cell dimension (Vegard's rule), skipping microscale thermoanalytical methods.[5,16]

A greater weight loss designates a proportionately larger carbon content replacing nitrogen atoms (for the TiN–C system) or C/N (for the TiO_2–C system) at the non-metallic sublattice sites.

Thermodynamics and chemical reactions

Considering that one elemental constituent of TiCN, i.e. nitrogen, is gaseous in its standard state, the study of the thermodynamic stability of all phases involved plays a substantial role in the knowledge of the phenomena observed. In fact, the atmosphere of argon or nitrogen can shift the thermodynamic equilibria and strongly influences the evolution of reactants present during every intermediate stage of the chemical reactions in progress.

The reactions

$$\text{in flowing Ar: } TiN + (1 - X)C \rightarrow TiC_{1-X}N_X + 0.5N_2(g) \uparrow \text{ (HTS)}$$

$$\text{in flowing } N_2: 2TiO_2 + 2(3 - X)C + XN_2(g) \rightarrow 2TiC_{1-X}N_X + 4CO(g) \uparrow \text{ (CTC)}$$

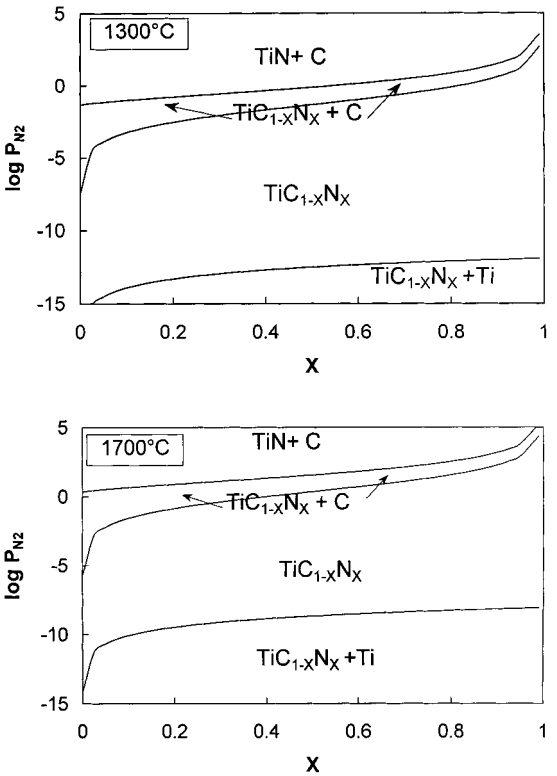

Figure 2 Examples of domains of stability of Raoultian $TiC_{1-X}N_X$ s.s at 1300 °C (a) and 1700 °C (b).

schematize the initial and final states of the high temperature synthesis (HTS) and of the carbothermal reduction–carbonitridation (CTC) being considered. On the hypothesis of full comsumption of the initial carbon in the starting mixture, the calculated weight losses in accordance with the mentioned reactions, are 11.6% and 50% respectively for HTS and CTC reactions. Concerning the HTS, the domains of stability of the $TiC_{1-X}N_X$ at various temperatures were calculated (Fig. 2) by adopting the theoretical model proposed by Pastor.[2] These diagrams allow us to define the range of nitrogen partial pressure permissible over the $TiC_{1-X}N_X$ in order to validate the proper experimental parameters for the synthesis and to prevent later its decomposition during sintering.

The boundary cases (Fig. 3) were also calculated from the Gibb's free energy functions.[17] This thermodynamic approach allowed us in advance to define an optimum temperature window to obtain TiCN. Under standard conditions, the nitridation of TiO_2 to TiN is favoured for temperatures above

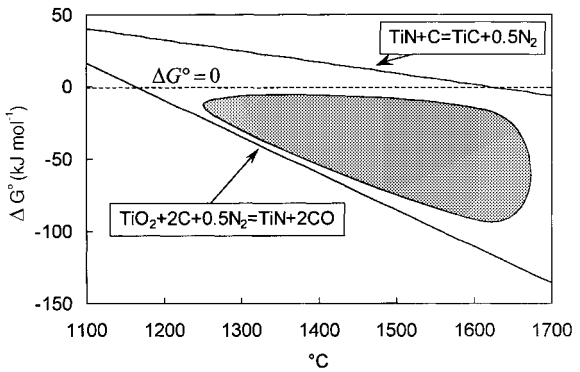

Figure 3 ΔG° *versus* temperature of the reactions written. The shadowed area locates an operational window to obtain TiCN. Thermodynamic calculations were performed with the HSC program package.[17].

1200 °C. On raising the temperature, TiC becomes stable and the residual carbon can react with TiN to form TiCN. The partial pressure of CO, released from the reacting interfaces, does not reach the equilibrium value because it is continuously removed by the nitrogen carrier gas, so the reduction can proceed further.

RESULTS

The most interesting results concerning the production of $TiC_{1-X}N_X$ powders are shown in Table 2. These data represent a selection of the tests performed after analyses of the reacted powders by XRD and SEM from both mixtures A and B.

XRD analyses, whatever the mixtures processed, detected systematically a set of peaks that could be assigned to an NaCl-type structured phase with a cell parameter that ranged from 0.4242 nm ($X = 1$, pure TiN) up to 0.4291 nm (namely $TiC_{1-X}N_X$ with $X = 0.4$). The XRD patterns collected with standard conditions (Fig. 4a) sometimes revealed, only after a smoothing — background subtraction — $K_{\alpha 2}$ stripping procedure, the existence of, at least, two stable $TiC_{1-X}N_X$ phases with distinct stoichiometries X_1 and X_2 (Table 2).

It has to be stressed that the evaluation of the X value may be difficult because of the line broadening of reflection peaks in the XRD patterns as a consequence of the extremely fine powdered samples used. By scanning the backreflection zone ($900 \leq 2\theta \leq 140\,^\circ$) with smaller angle steps and longer sampling times, a further detailed XRD pattern was acquired for a selected powder (Fig. 4b and c). The X_2 value was estimated from Equation 1 by extrapolating a_{TiCN} from the interplanar spacings d_{hkl} calculated from the maximum height of the reflection peaks (Fig. 4c). Moreover, weaker peaks overlap each other as a sort of compositional continuum of TiCN phases (Fig. 4c, see the arrow), and are likely associated with different stoichiometries.

Figure 5 shows the morphology of the reacted powders A-C1 (a) and B-C1 (b): both result in

Table 2 Experimental conditions and microstructural parameters of the most interesting reaction products[a]

Mixture	T (°C)	t (min)	X_1	X_2	Weight loss (%)	I_{X_2}/I_{X_1}	Notes
TiN + 10 wt% C (flowing argon)							
A-C1	1350	180	0.75	0.4	14.3	<1	—
A-C1	**1430**	**180**	**0.55**	**0.45**	**17.0**	**>1**	*
A-C2	1350	180	>0.9	0.6	14.8	~1	*
A-C2	1400	180	0.6	0.45	16.7	≫1	—
A-C3	1350	120	0.8	—	14.4	—	—
A-C3	1400	120	0.85	0.65	14.4	<1	*
TiO_2 + 27 wt% C (flowing nitrogen)							
B-C1	1450	240	0.8	—	42.0	—	
B-C1	1500	120	>0.95	0.8	42.6	~1	*
B-C1	**1500**	**180**	**0.3**	—	**43.0**	—	*
B-C2	1450	240	>0.95	—	41.4	—	—
B-C2	1500	180	1	0.7	41.8	<1	*
B-C3	1500	120	0.75	—	44.8	—	—

[a] T: isothermal temperature; t: holding time; I_{X_1},I_{X_2}: intensity of the (220) peak relative to X_1 and X_2 values;
* Broadened peaks.

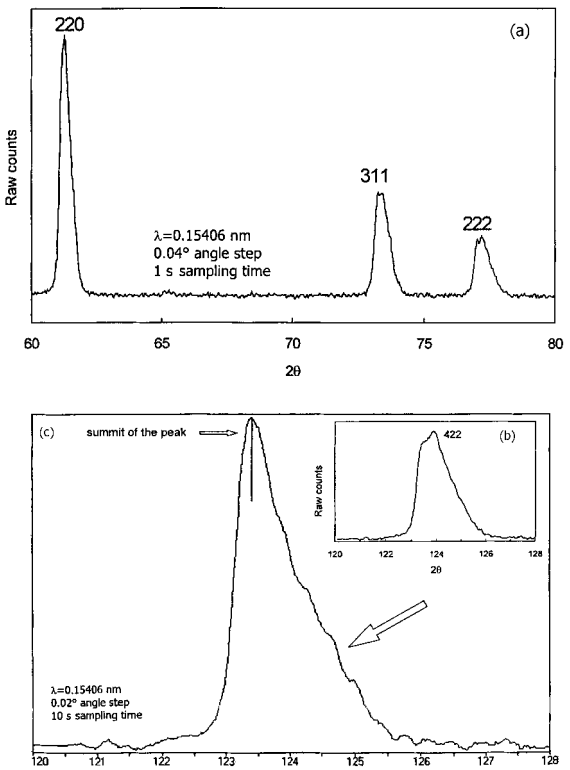

Figure 4 XRD patterns from sample AC-1 (1430 °C for 180 min) for different 2θ ranges. Both (a) and (b) are unprocessed patterns, whereas (c) is the output after a processing routine.

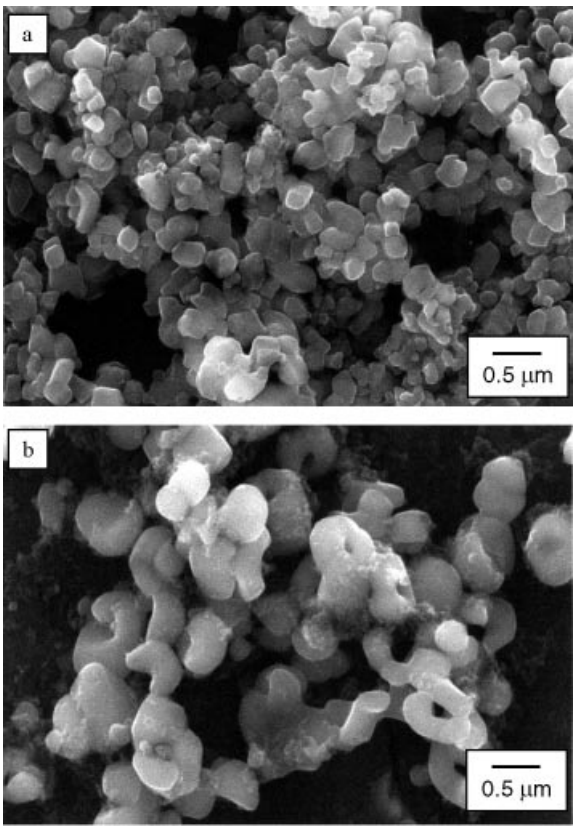

Figure 5 SEM micrographs of the morphology of the as-treated mixture AC-1 (a) and BC-1 (emboldened in Table 2).

submicrometric $TiC_{1-X}N_X$, but the former is finer than the latter. The specific surface area of AC-1 and the residual oxygen results were 4.9 $m^2\ g^{-1}$ and <1 wt% respectively.

As stated before, greater weight losses are related to cycles in which the reaction considered progressed further.

DISCUSSION

The carburization of TiN

The carburization of TiN under flowing argon occurred after direct interaction between carbon and TiN itself. During the reaction, the carbon atoms, owing to their comparable atomic radii, entered into the TiN lattice, filling vacancies or substituting nitrogen at non-metal sublattice sites.

At the operating nitrogen pressure ($\ll$1 atm), TiN/C mixtures are thermodynamically unstable and react readily (Fig. 2). The inward diffusion of carbon atoms, as well as the outward diffusion of nitrogen atoms, influence the reaction rate of the synthesis and, of course, are related to the equilibrium solubilities of carbon and nitrogen in the TiCN lattice at that temperature.

The effects of experimental parameters (i.e. temperature–time, green density, pressure and flow) on the reactions involved can be described as follows.

Firstly, temperature is the main influencing factor of the reaction (Fig. 6). Moreover, temperatures higher than 1500 °C certainly enabled us to obtain single $TiC_{1-X}N_X$ with X close to 0.5 (Fig. 6), but that product presents necking–facetting and widespread agglomeration; unfortunately, grain size deviated from the planned target for fineness. Among the types of carbon used, C-1 and C-3 exhibited similar reactivity, but much residue of C-3 remained in the final product.

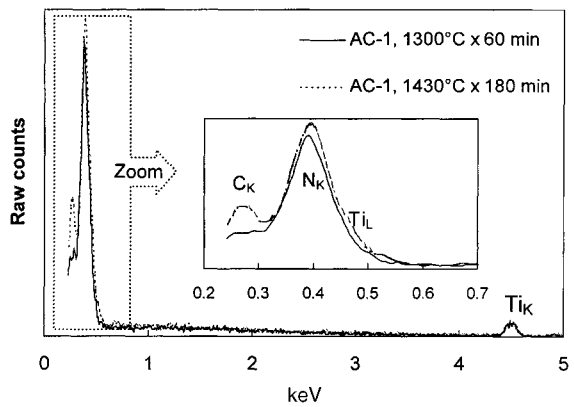

Figure 6 Windowless energy-dispersive spectra (incident beam energy 6 keV) from two as-treated mixtures. Increasing the temperature and time results in a faster incorporation of carbon atoms.

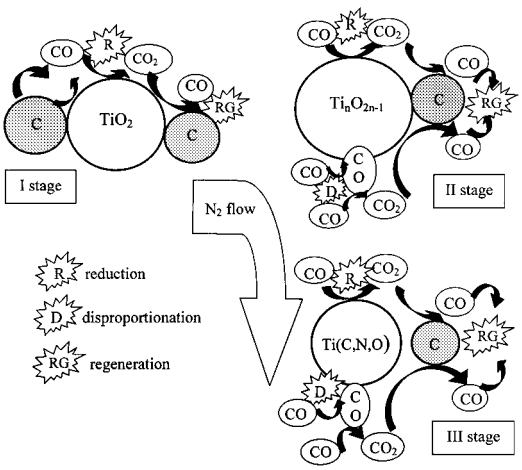

Figure 7 Model of CTC of TiO_2. The scheme has been adapted from the model proposed by Berger *et al.*[1].

Secondly, the surface of the sample exposed to the (flowing argon) atmosphere and the green density of the pellet influence the kinetics. In fact, the former limits the escape of gaseous species from the bulk under reaction and probably changes the local nitrogen partial pressure, whereas the latter enhances the contact area among the reactants. In fact, it was ascertained that, starting from pellets with poorer green density, both weight loss and X values were lower than those indicated in Table 2.

With reference to the weight loss data (Table 2), every mixture processed had a weight loss greater than that calculated (i.e. 11.6%). At very low nitrogen partial pressures, and for temperatures higher than 1300 °C, TiN is known to release nitrogen[4] and suffer a weight loss. A preliminary thermal test on only TiN powder (1500 °C, flowing argon, graphite crucible) confirmed a weight loss of 7%. After taking into account the additional contributions from the volatilization of impurities (Table 1) and from adsorbed species on the particle surface, the measured weight losses are in agreement with the calculated stoichiometries of TiCN.

The best experimental conditions to obtain fine, regularly shaped and scarcely agglomerated particles (Fig. 5a) are highlighted in Table 2.

CTC of TiO_2

Figure 7 presents a model of the CTC of TiO_2. The sequence of the intermediate transformations had been confirmed experimentally[1] and can be fairly described as follows:

$$TiO_2 \rightarrow Ti_nO_{2n-1} \rightarrow Ti_3O_5 \rightarrow TiC_XN_YO_Z$$

The main mass transport is realized over the gas phase by the CO/CO_2 couple. Details of the model are reported elsewhere.[1] Diverse opinions can be found in the literature about the final stages of the reactions[1,2,5,7,8,18] because of the lack of standardized experimental conditions. The stream of nitrogen gas and the constant removal of CO, for example, prevent a real achievement of thermodynamic equilibrium and create an 'open system'. In any case, mechanisms and reaction yield depend on several parameters: temperature and time, pressure and flow of gas, types of raw constituent (TiO_2, TiN, carbon), particle size–porosity–purity, diffusion rate of the moving species, volatility of the intermediate reactants.[1,2,5,7,8,18] An excess of carbon in the starting mixture ($C:TiO_2 > 2.5$ mol%) and a stronger nitrogen flow, for example, enhance the kinetics to obtain a better reaction yield.[3] In fact, the former enlarges the contact area, whereas the latter shortens the path for outgoing oxygen and incoming carbon/nitrogen and lowers the equilibrium constants.

The melting temperatures T_M of the Magneli phases (Ti_nO_{2n-1}, $4 \leq n \leq 10$) are lower than that of TiO_2 (rutile or anatase), so, in heating up the sample, grain growth took place. After the appearance of cubic Ti(C,N,O), independently of the nitrogen partial pressure, T_M rose rapidly and

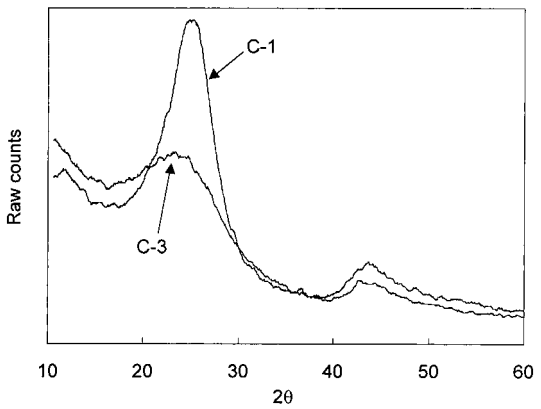

Figure 8 XRD patterns of carbon black C-1 and active carbon C-3.

inhibited further grain growth. The simultaneous carbonitridation seemed to slow down sintering and suppress grain growth of the intermediate cubic Ti(C,N,O).[1,3]

It should be noted that Magneli phases are substoichiometric titanium oxides rich in vacancies, so they can easily accomodate carbon (after reduction or disproportionation) and nitrogen (substitution) within the crystal lattice (Fig. 7). The progressive reduction of intermediate oxides can be fed only with an immediate regeneration of CO.[1] Thus the reactivity of carbon with CO_2, directly related to its structure, represents an important influencing factor on the reaction yield, i.e. the final content of carbon, nitrogen and oxygen.

Among the types of carbon tested active carbon C-3 has an organic origin and is characterized by a non-ideal porous structure, whereas carbon black (C-1, C-2) is a finely dispersed type of carbon that is not very porous. The reactivity of carbon should be empirically interpreted, not only in terms of graphitization (Fig. 8) and specific surface area (Table 1), but also by considering the oxygen bonded with surface functional groups decomposing at higher temperatures. The latter are much more prevalent on the surface of C-3 than C-1 and C2. This feature helps the reaction to start at lower temperatures. The presence of coarse platelike particles in active carbon C-3 (Fig. 1e) prevented us obtaining carbon-free TiCN powder, although the reaction yield reached very encouraging levels.

Figure 5b shows the mixture B-C1 (Table 2). This example represents the best compromise of the required characteristics after processing. Indeed the high temperature (1500 °C) triggered grain growth, negating our efforts to obtain an ultrafine TiCN product.

The essential condition to convert titania completely to TiCN remains, in any case, an intimate TiO_2/C contact. Moreover, lacking a continuous supply of CO for titania reduction and of carbon for CO regeneration can lead to detrimental effects on the CTC reaction, such as agglomeration and grain growth: reaction products with different size, shape and purity will result.

CONCLUSIONS

Starting from blends of nanosize commercial TiN or TiO_2 powders mixed with different carbon powders (two carbon blacks, one active carbon), the study sets up a low-cost route to produce fine $TiC_{1-X}N_X$ powders with an X value close to 0.5. For the compositions TiN + 10 wt% C and TiO_2 + 27 wt% C, six different mixtures (three each for TiN and TiO_2) were prepared and treated in the temperature range 1300–1700 °C under argon and nitrogen atmosphere, respectively, for TiN- and TiO_2-based mixtures. On the basis of thermodynamic calculations, the domains of TiCN stability were calculated. Screening the product characteristics by means of XRD and SEM inspections, the most interesting results were reported and discussed. The mixture TiN–10 wt% C, treated at 1430 °C for 180 min in flowing argon, had submicrometric regularly shaped particles and $X \approx 0.5$. With reference to mixture TiO_2–27 wt% C, heated at 1500 °C for 180 min in flowing nitrogen, grain growth took place, although the grain size was still submicrometric and the X value reached ~0.3. The features of the products were correlated to the mechanisms involved during the reaction. Models of the carburization of TiN and of the CTC of TiO_2 were also proposed.

Acknowledgements This work was supported by MURST and CNR under the National Project 'Innovative Materials', Law 95/95–5%. The authors would like to thank Dr G. Celotti (IRTEC–CNR) for his helpful contribution on XRD analyses and Mr D. Dalle Fabbriche for assistance on furnaces.

REFERENCES

1. Berger L-M, Gruner W, Langholf E, Stolle S. *Int. J. Refract. Met. Hard Mater.* 1999; **17**: 235.

2. Pastor H. *Mater. Sci. Eng. A* 1988; **105–106**: 401.
3. Jha A, Yoon SJ. *J. Mater. Sci.* 1999; **34**: 307.
4. Ettmayer P, Kolaska H, Lengauer W, Dreyer K. *Int. J. Refract. Met. Hard Mater.* 1995; **13**: 343.
5. Ličko T, Figusch V, Púchyová J. *J. Eur. Ceram. Soc.* 1989; **5**: 257.
6. Shaviv R. *Mater. Sci. Eng. A* 1996; **209**: 345.
7. Li W-Yu, Riley FL. *J. Eur. Ceram. Soc.* 1991; **8**: 345.
8. White GV, Mackenzie KJD, Brown IWM, Bowden ME, Johnston JH. *J. Mater. Sci.* 1992; **27**: 4294.
9. Berger L-M, Ettmayer P, Schultrich B. *Int. J. Refract. Met. Hard Mater.* 1993–94; **12**: 161.
10. Koc R, Folmer JS. *J. Mater. Sci.* 1997; **32**: 3101.
11. Ahlén N, Johnsson M, Nygren M. *J. Mater. Sci. Lett.* 1999; **18**: 1071.
12. Yoshimura M, Nishioka M, Somiya S. *J. Mater. Sci. Lett.* 1987; **6**: 1463.
13. Preiss H, Berger L-M, Schutze D. *J. Eur. Ceram. Soc.* 1999; **19**: 195.
14. Levi G, Kaplan WD, Bamberger M. *Mater. Lett.* 1998; **35**: 344.
15. Azaroff LV, Buerger MJ. *The Powder Method*. McGraw-Hill: New York, 1958; 238.
16. Gruner W, Stolle S, Berger L-M, Wetzig K. *Int. J. Refract. Met. Hard Mater.* 1999; **17**: 227.
17. Roine A. HSC Chemistry 2.0. Outokumpo Research Oy: Finland, 1994.
18. Tristant P, Denoirjean-Deriu P, Lefort P. *Third Euro-Ceramics*, vol. 1, Duran P, Fernandez JF (eds). Faenza Editrice Iberica S.L.: 1993; 1091.

